THE ASTROPHYSICAL JOURNAL, 329:882–893, 1988 June 15

RELATIONS BETWEEN BROAD-BAND LINEAR POLARIZATION AND Ca II H AND K EMISSION IN LATE-TYPE DWARF STARS

JUHANI HUOVELIN[1] AND STEVEN H. SAAR
Joint Institute for Laboratory Astrophysics, University of Colorado and National Bureau of Standards
AND
ILKKA TUOMINEN
Observatory and Astrophysics Laboratory, University of Helsinki, Finland
Received 1987 November 9; accepted 1987 December 10

ABSTRACT

We compare broad-band *UBV* linear polarization observations of a sample of late-type (F5–K5) dwarfs with contemporaneous measurements of Ca II H and K line core emission. Various parameters representing the degree of polarization are studied in relation to chromospheric activity. A weighted average of the largest values of the polarization degree appears to be the best parameter for activity diagnostics. Linear polarization is extremely sensitive to differences in the surface distribution of active areas, and thus shows considerable scatter when plotted against other activity indicators, such as the relative Ca II emission flux R_{HK}' and the inverse Rossby number. Nevertheless, evidence of an increase with activity can be seen. The average maximum polarization in the ultraviolet shows significant increase from late-F to late-G stars. The small polarization observed in even highly active F stars is possibly due to lack of large scale surface inhomogeneities on these stars.

Polarization in the *U* band is considerably more sensitive to activity variations than that in the *B* or *V* bands. Power-law fits indicate a wavelength dependence varying from $\lambda^{-1.0\pm1.0}$ (most inactive stars) to $\lambda^{-5.9\pm0.6}$ (ξ Boo A). For several stars, the disagreement with Rayleigh scattering (λ^{-4}) is large. We suggest stellar magnetic fields and the resulting saturation in the Zeeman-sensitive absorption lines to be the most probable source of linear polarization in late-type main-sequence stars, consistent with the weak trend found with Ca II flux and with inverse Rossby number.

The analysis of short term variability in nearly simultaneous polarimetric and Ca-emission observations of ξ Boo A and HD 206860 suggests at least three active areas on both stars.

Subject headings: Ca II emission — polarization — stars: late-type — stars: magnetic

I. INTRODUCTION

Broad-band linear polarization connected with solar magnetic regions was first discovered nearly 20 years ago (Dollfus 1958; Leroy 1962). More recently, linear polarization has been observed in other late-type dwarfs as well (Piirola 1977; Tinbergen and Zwaan 1981; Huovelin *et al.* 1985). The source of linear polarization on stars is somewhat unclear, however, due to possible contribution from Rayleigh scattering (e.g., Piirola and Vilhu 1982). The average degree of polarization appears to depend on the chromospheric activity level of the star and follows the short period changes in activity caused by rotational modulation, suggesting a magnetic origin (see Huovelin *et al.* 1986). The variations, as well as the mean degree of linear polarization, are usually very small ($<0.1\%$, Piirola 1977; Tinbergen and Zwaan 1981; Huovelin *et al.* 1985), and as a result conclusive evidence for a connection between linear polarization, magnetic fields, and chromospheric activity has not yet been found.

The observed increase of linear polarization toward short wavelengths (Huovelin *et al.* 1985) does not contradict either the magnetic or Rayleigh scattering model. The increase in the number of saturated, magnetically sensitive absorption lines toward short wavelengths could cause the observed wavelength dependence (Kemp and Wolstencroft 1974; Calamai, Landi Degl'Innocenti, and Landi Degl'Innocenti 1975; Landi Degl'Innocenti *et al.* 1981; Tinbergen and Zwaan 1981; Landi Degl'Innocenti 1982), but a qualitatively similar effect could be produced by simple Rayleigh scattering in the optically thin part of the stellar atmosphere (degree of polarization $\propto \lambda^{-4}$). Magnetic intensification in the saturated Zeeman-sensitive lines will arise from stellar spots and plages, while the scattering could take place in optically thin disks or other inhomogeneities above the stellar surface (Piirola and Vilhu 1982). The phase of the maximum polarization will, however, not be the same in these two cases (e.g., Saar and Huovelin 1988). In both cases, however, we expect rotational modulation of linear polarization, with variations depending on the inclination of the star, and the distribution and sizes of polarizing areas.

Rotational modulation of Ca II emission (Vaughan *et al.* 1981) has been successfully used in determinations of rotation periods for 41 late-type dwarfs and subgiants (Baliunas *et al.* 1983; Noyes *et al.* 1984). In the simplest case, a single active region will produce the highest level of chromospheric emission when it crosses over the disk center. If the linear polarization is due to magnetic fields, it will likely be spatially associated with the Ca II emission. There will, however, be a phase lag of ~ 0.125 between the peak Ca II emission and the peak linear polarization due to their different angular dependencies (see § III). Simultaneous measurements of linear polarization and Ca II emission can therefore give complementary information on the spatial distribution of magnetic

[1] On leave from the Observatory and Astrophysics Laboratory, University of Helsinki, Finland.

regions, although the situation is difficult to interpret for all but the simplest geometries.

In the present paper, we analyze broad-band *UBV* linear polarimetry and Ca II (H + K) emission observations for a sample of late-type dwarfs, comparing the results with stellar parameters, models of linear polarization (Saar and Huovelin 1988), and with a simple spot model described here. On the basis of the results, we also give suggestions for future observations.

II. OBSERVATIONS

The polarimetric observations were made in four periods, 1985 August 16–26, 1985 September 26–October 6, 1986 June 17–22, and 1986 September 10–18, using the 1.25 m telescope of the Crimean Astrophysical Observatory, with a multichannel version of the double image chopping polarimeter of the University of Helsinki (Piirola 1973, 1975). Earlier observations from years 1983 and 1984 (see Huovelin *et al.*. 1985) were combined into the averages. The observations were made simultaneously in three passbands (close to Johnson *UBV*),with effective wavelengths 0.36, 0.44, and 0.53 μm, respectively. The instrumental polarization was obtained from observations of polarimetric standard stars each night during the observing run. At least three small polarization standard stars (e.g., Piirola 1977) were used in the instrumental polarization determinations during each observing run, and the position angle was corrected using observations of a highly polarized standard star (e.g., Hsu and Bregel 1982). The standard error in all instrumental polarization measurements was less than 0.02% in *U* and less than 0.01% in *B* and *V*. The instrumental polarization is constant, to high precision, during a single observing run up to at least 14 nights; hence, the probability of spurious temporal variations caused by the instrument is low. After corrections for instrumental effects, weighted nightly averages were calculated for each star from at least three individual observations, except one night for HD 20630 (two observations on 1986 September 17–18), and one night for ξ Boo A (two observations on 1986 June 17–18). Our sample, consisting of nearby stars, should have only a minor contribution from interstellar polarization (e.g., Piirola 1977).

The Ca II (H + K) observations are nightly averages from the *S*-index measurements at Mount Wilson, obtained with the Ca II (H + K) photometer at the 60 inch (1.5 m) telescope of the Mount Wilson Observatory (Vaughan, Preston, and Wilson 1978). We converted the *S*-index values into chromospheric Ca II (H + K) flux measures (F_{HK}') with the method described in Noyes *et al.* (1984). However, the conversion factor, C_{cf}, as well as the basal flux subtracted from the total flux, differ from those in Noyes *et al.* (1984). We used the $C_{cf}(B-V)$ function recalibrated by Rutten (1984), and the basal flux was obtained from tables for main-sequence stars of Rutten and Schrijver (C. J. Schrijver, private communication). For T_{eff} versus $B-V$ dependence we employed the calibration of Böhm-Vitense (1981) for main-sequence stars (third-order polynomial fit to the tabulated values). All excess fluxes were multiplied by factor 1.6×10^6 (appropriate for dwarfs and valid only for the excess line core emission; Schrijver *et al.* 1988), leading to flux values close to units ergs cm^{-2} s^{-1}. The respective formulae are

$$F_{HK}' = 1.6 \times 10^6(10^{-14} S C_{cf} T_{eff}^4 - F_{0,HK}) , \quad (1)$$

where

$$\log (C_{cf}) = 0.24 + 0.43(B-V) - 1.33(B-V)^2 + 0.25(B-V)^3 \quad (2)$$

$$\log (F_{0,HK}) = 1.83 - 2.76(B-V); \; 0.3 < (B-V) < 0.48 \quad (3)$$

$$\log (F_{0,HK}) = 7.79 - 2.23(B-V); \; 0.48 < (B-V) < 1.25 \quad (4)$$

$$\log (T_{eff}) = 4.04 - 0.71(B-V) + 0.55(B-V)^2 - 0.20(B-V)^3; \; 0.3 < (B-V) < 1.5 , \quad (5)$$

where $F_{0,HK}$ represents the minimum (basal) flux. The excess fluxes can then be converted to relative fluxes $R_{HK}' = F_{HK}'/(\sigma T_{eff}^4)(\sigma = 5.67 \times 10^{-5}$ ergs cm^{-2} s^{-1} K^{-4}). The program stars with Ca II emission data are listed in Table 1.

III. RESULTS AND DISCUSSION

a) *Correlations of Average Values*

We studied correlations between the long-term averages in Ca II emission and linear polarization using several alternatives for representative parameters in both quantities. For Ca II emission, we tried the average normalized and unnormalized fluxes ($\langle R_{HK}' \rangle$ and $\langle F_{HK}' \rangle$), the standard deviations of R_{HK}' and F_{HK}' from the scatter between nightly averages, the amplitudes of variations of these fluxes (i.e., largest minus smallest value during the observations), and finally, the empirical Rossby number $R_0 = P_{rot}/\tau_c$, where P_{rot} is the rotation period, and the convective turnover time τ_c was obtained from the empirical formula in Noyes *et al.* (1984). The respective parameters for linear polarization were the average of polarization $\langle P \rangle = (\langle P_x \rangle^2 + \langle P_y \rangle^2)^{0.5}$, the standard deviation of *P* from the scatter between nightly averages, and the average of the most significant deviations from zero [P_s =

TABLE 1

PROGRAM STARS AND Ca II H AND K EMISSION DATA[a]

HD	Name	Spectral Type	$B-V$	P_{rot}	$\langle S \rangle$	Time of Observation	N
1835	9 Cet	G2 V	0.66	7.7	0.321	6338–6430	27
20630	κ Cet	G5 Vv	0.68	9.4	0.342	6300–6490	58
25998	50 Per	F7 V	0.46	2.6	0.278	6330–6370	16
126053	...	G3 V	0.63	21.1	...	...	...
131156A	ξ Boo A	G8 V	0.76	6.2	0.442	6157–6640	163
143761	ρ CrB	G2 V	0.60	19.7	0.154	6275–6305	19
185144	σ Dra	K0 V	0.79	...	...	...	...
194012	...	F5 V	0.51	6.8	0.195	6275–6375	49
201091	61 Cyg A	K5 V	1.18	37.9	0.537	6280–6645	57
206860	...	G0 V	0.58	4.7	0.333	6278–6375	50

[a] Times of observations are JD −2,440,000, and *N* is the number of observing nights.

TABLE 2

Ca II H + K Average Fluxes $\langle F_{HK}' \rangle$ and $\langle R_{HK}' \rangle$ and Related Activity Parameters for the Program Stars[a]

HD	log $\langle F_{HK}' \rangle$	log $\langle R_{HK}' \rangle$	log σ_F	log σ_R	log A_F	log A_R	log R_0
1835	6.552	−4.227	5.217	−5.562	5.474	−5.305	−0.213
20630	6.559	−4.201	5.270	−5.490	5.608	−5.152	−0.164
25998	6.791	−4.212	5.170	−5.833	5.418	−5.585	−0.027
126053	...	...	...	...	...	...	0.290
131156A	6.566	−4.122	5.299	−5.389	5.699	−4.989	−0.458
143761	5.848	−4.991	4.775	−6.065	5.119	−5.720	0.336
194012	6.347	−4.593	5.222	−5.718	5.568	−5.372	0.172
201091	5.715	−4.619	4.389	−5.945	4.904	−5.430	0.191
206860	6.721	−4.139	5.556	−5.305	5.891	−4.969	−0.230

[a] σ_F and σ_R are the standard deviations (i.e., night-to-night scatter) in F_{HK}' and R_{HK}', A_F, and A_R are the half-amplitudes of the flux variations, and R_0 are the Rossby numbers.

$\langle (P_x^2 + P_y^2)^{0.5} \rangle$, where $P > 2\sigma_P$], in each passband (UBV). To avoid ill-defined averages, only those stars with more than two nights of polarimetric observations were used. The errors in the polarization averages are either the weighted errors from the dispersion of points or the mean errors of the individual points; in each case the larger one of these errors was chosen. Our definition of P_s correctly determines the degree of linear polarization for stars with a large net P. It will, however, tend to overestimate P_s for stars with very small true polarization, since it will identify noise spikes greater than $2\sigma_P$ as true signal. We believe that the correct estimate for P_s on stars with nonzero P compensates for this fault. The various averages and amplitudes are listed in Tables 2 and 3.

The best correlations were obtained between P_s and R_0 (Fig. 1). Due to the small size of our sample (nine stars) the trends found in the analysis are only suggestive. $P_s(U)$ shows evidence for an increase with increasing activity (i.e., decreasing Rossby number), with $P_s(U) \propto R_0^{-0.08 \pm 0.02}$. Part of the scatter in the polarization likely results from different surface distributions of active areas on the observed stars. Two active stars, HD 20630 (κ Ceti) and HD 206860, show very low degrees of polarization, suggesting partial cancellation due to several active areas scattered over the stellar surface (Landi Degl'Innocenti 1982; Saar and Huovelin 1988). The scatter in R_0 versus $P_s(U)$ may also be partly due to the dependence of the maximum linear polarization on spectral type, with larger P_s expected for later spectral types caused by increased line blanketing (see § III*b*).

The slopes in the B and V bands are closer to zero [$P_s(B) \propto R_0^{-0.02 \pm 0.01}$ and $P_s(V) \propto R_0^{-0.02 \pm 0.01}$], indicating that $P_s(U)$ is the best of the three linear polarization measures for use as an activity indicator in late-type stars. The P_s versus $\langle R_{HK}' \rangle$ distribution (Fig. 2) is similar to P_s versus R_0, as expected, since R_0 and R_{HK}' are strongly correlated (Noyes *et al.* 1984). The other parameters did not show clear functional dependencies, and in the following, we will suggest some reasons for the lack of correlations.

The averages of Ca II emission in absolute flux units (i.e., units of F_{HK}') show even larger scatter as functions of polarization than those in relative units (R_{HK}'). This is probably because polarization, like R_{HK}', is a *relative* measure of activity (polarization is calculated using *normalized* Stokes parameters). We do not expect to find a simple relation between rotation period and linear polarization, because the

TABLE 3

Stellar Polarization Parameters

Parameter	HD 1835	HD 20630	HD 25998	HD 126053	HD 131156A	HD 143761	HD 185144	HD 194012	HD 201091	HD 206860
$\langle P(U) \rangle$[a]	29	9	18	83	194	25	35	12	3	6
σ_u[b]	85	49	39	78	74	36	59	46	79	40
M.E.(U)[c]	11	9	7	25	21	10	9	6	8	6
$\langle P(B) \rangle$[a]	11	10	22	47	34	10	27	26	16	30
σ_B[b]	45	25	22	47	14	15	31	17	22	26
M.E.(B)[c]	7	4	4	16	5	6	7	3	3	3
$\langle P(V) \rangle$[a]	3	11	10	14	40	7	19	9	13	6
σ_V[b]	34	28	16	10	29	17	29	27	27	33
M.E.(V)[c]	6	3	4	7	6	5	7	5	3	3
N[d]	14	15	11	3	5	7	6	14	17	20
$P_s(U)$[e]	155	69	40	103	189	78	63	46	87	63
Error	17	18	6	23	16	18	13	6	9	10
$P_s(B)$[e]	55	36	33	84	40	36	55	36	30	39
Error	9	10	3	26	4	11	32	7	2	3
$P_s(V)$[e]	49	32	26	13	42	25	41	33	28	30
Error	8	5	5	5	5	8	8	8	3	4

Note.—Units: 0.001%.

[a] $\langle P \rangle = (\langle P_x \rangle^2 + \langle P_y \rangle^2)^{0.5}$.

[b] Standard deviation of P from night-to-night variations.

[c] Standard mean error.

[d] Number of nights observed.

[e] $P_s = \langle (P_x^2 + P_y^2)^{0.5} \rangle$, where $P > 2\sigma_P$.

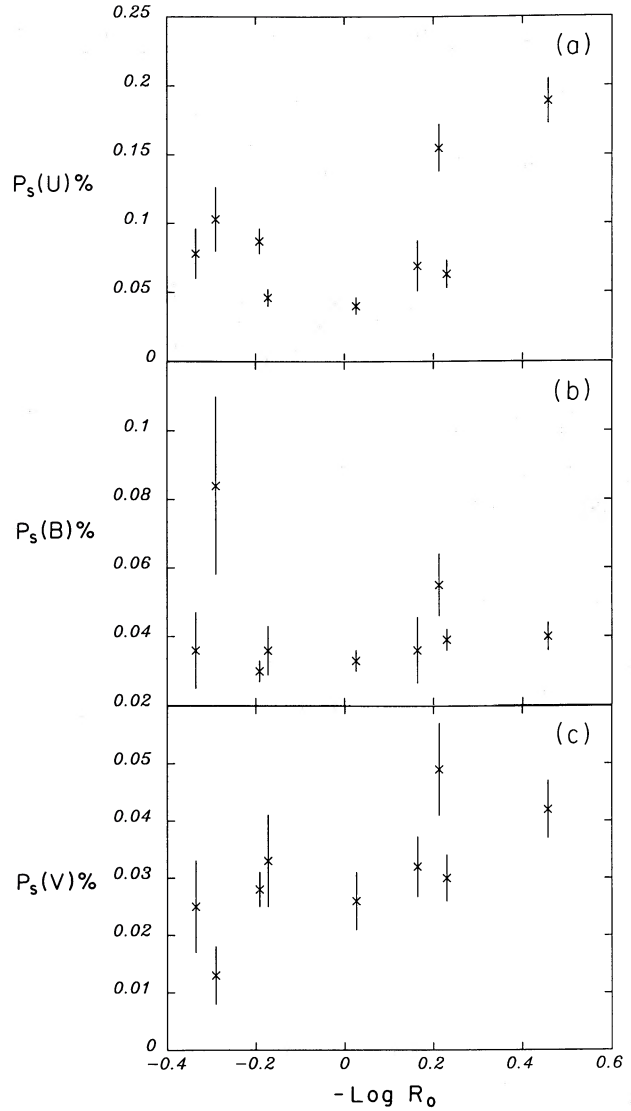

FIG. 1.—Average linear polarization P_s vs. logarithm of inverse Rossby number R_0, in (*a*) *U*, (*b*) *B*, and (*c*) *V* band. Error bars here and in all subsequent figures are $\pm 1\ \sigma$.

degree of linear polarization also depends strongly on the stellar magnetic area geometry (Landi Degl'Innocenti 1982), which is time-dependent, and may also be a function of spectral type (e.g., Giampapa and Rosner 1984). The mean degree of polarization $\langle P \rangle$, as derived from the average Stokes parameters $\langle P_x \rangle$ and $\langle P_y \rangle$, will also be a poor indicator of activity if the observations have been made at random rotational phases. Consider, for example, a pole-on star with constant active areas on its surface. The degree of polarization will be constant (P_0) during rotation, but the computed average $\langle P \rangle$ will tend toward zero with increasing number of observations (Landi Degl'Innocenti 1982), since all pairs of P_x and P_y observations differing by 0.25 in phase will cancel out (P_x and P_y change sign with a 90° rotation). This same example also demonstrates why P_s is a better measure of activity, since it would yield $P_s \approx P_0$, independent of the number of observations.

One might assume that the peak-to-peak amplitude of short-term Ca II emission variations (i.e., the rotational modulation) would correlate well with the amplitude of linear polarization variations. This is not the case, however, since the rotational variability of chromospheric Ca II emission is qualitatively different from that of linear polarization. Ca II emission measurements contain positive contributions from all the visible active areas, while linear polarization can suffer substantial cancellation depending on the distribution of active areas on the stellar surface.

The stellar orientation relative to the observer is also important. Consider another simple case, a star with only one active region on the stellar equator. For this case we would obtain different peak-to-peak amplitudes of Ca II emission variations for similar stars with different inclinations (amplitude $\propto \sin i$). With decreasing inclination, the maximum degree of linear polarization remains unchanged, with only the direction and the phase of maximum being changed, until the inclination reaches a critical value (see Fig. 3). The critical stellar inclination angle for equatorial magnetic regions is between 45° and

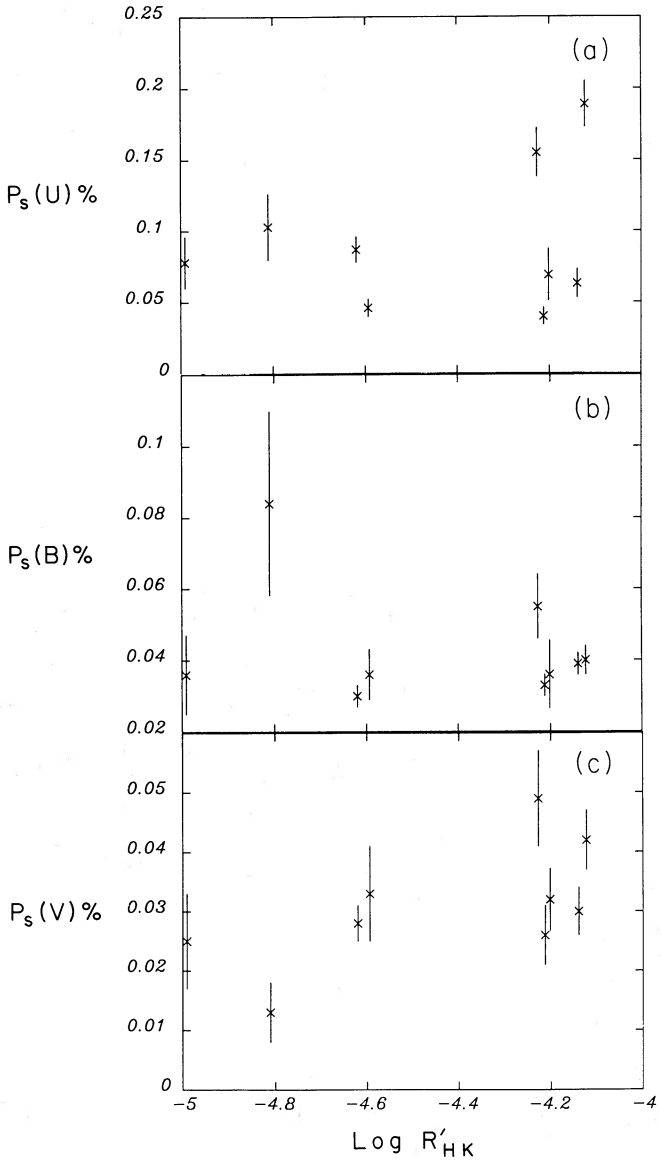

FIG. 2.—P_s vs. log of relative Ca II flux R_{HK}', in (*a*) *U*, (*b*) *B*, and (*c*) *V*

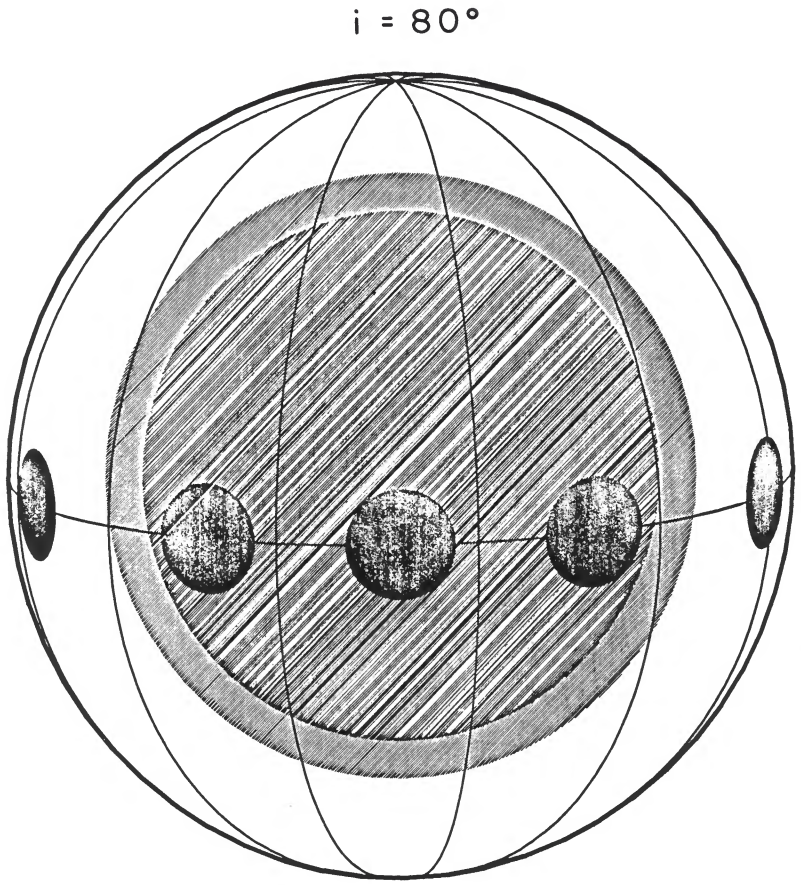

FIG. 3*a*

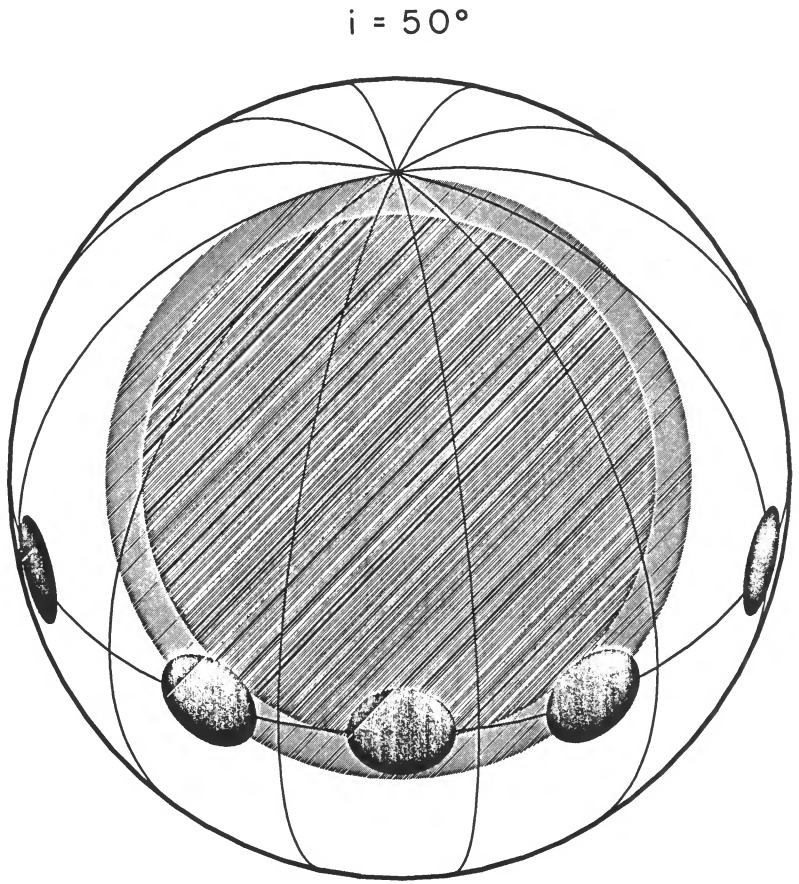

FIG. 3*b*

FIG. 3.—Schematic presentation of an equatorial polarizing area moving across the visible stellar disk (*small dark circles*), with three different inclinations, (*a*) 80°, (*b*) 50°, and (*c*) 30°. In (*a*) and (*b*), active area crosses the central part of the disk (*shaded area*), and magnetic intensification causes equal maximum degree of polarization at the outer boundary of the shaded area (two maxima per rotation; phase separation different in (*a*) and (*b*). In (*c*), the maximum polarization is smaller). The outer shaded ring shows the uncertainty in limb darkening.

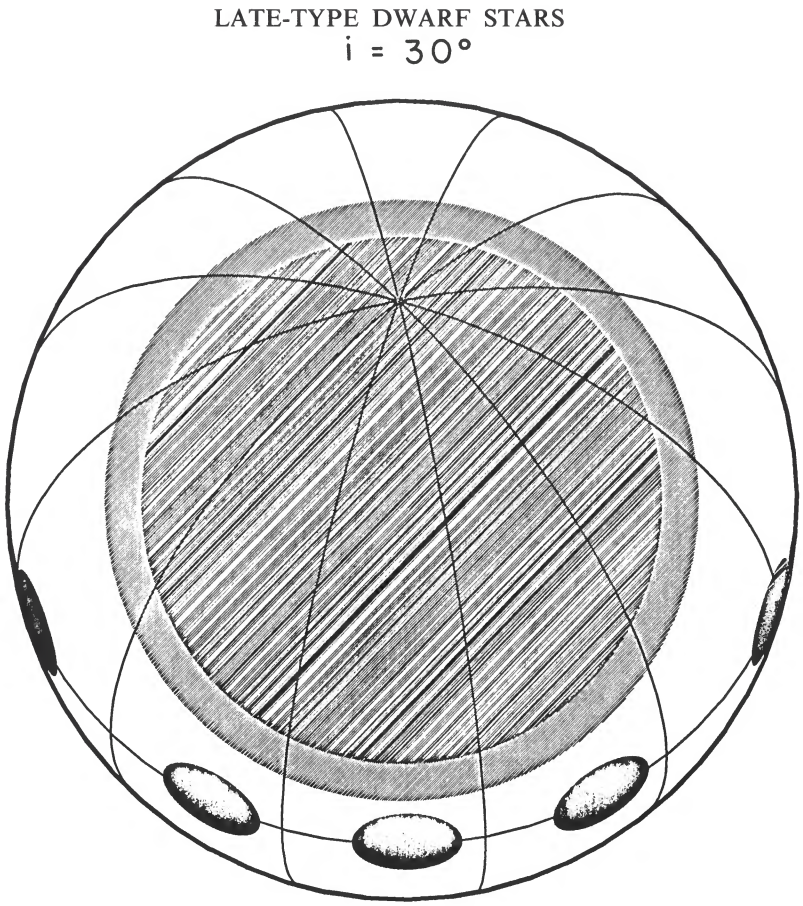

FIG. 3c

35°, corresponding to situations from full limb-darkening to complete absence of limb-darkening (Unno 1956; Saar and Huovelin 1988), and 0° for simple scattering. Thus, without knowledge of the distribution of active areas and the inclination of the star, it is impossible to predict the relationship between the amplitude of linear polarimetric variations and the amplitude of Ca II emission variations. The standard deviations (i.e., the scatter of nightly averages) behave similarly and are thus also poor parameters in comparisons between Ca II emission and linear polarization.

The Ca II modulation itself can also be misleading. The excess Ca II flux shows rotational variations of typically ~5%–30% (Noyes *et al.* 1984). It is not clear how much the modulation amplitude is depressed by "overlapping" active regions (i.e., at least one active region always at visible disk) and/or a ubiquitous background (i.e., the stellar analog of solar chromospheric network). The homogeneous background emission itself might vary in time (e.g., Schrijver 1988) and have no direct effect on variations in the integrated linear polarization. Thus, there are several reasons to expect the amplitudes of Ca II emission and linear polarization not to be simply correlated.

b) Spectral Type Dependence of Polarization

We plotted P_s against $B-V$ color in order to study the possible spectral type dependence of polarimetric variations. The distribution in the U band (see Fig. 4) indicates increasing linear polarization toward later spectral types from $B-V = 0.46$ to 0.76, consistent with trends observed by Piirola (1977) and Tinbergen and Zwaan (1981). The discrepant star in this interval, κ Ceti ($B-V = 0.68$), again suggests a possible partial cancellation effect that shifts an active star down in the diagram. HD 206860 ($B-V = 0.58$), however, fits the increasing trend. Since we have only two stars of spectral types later than G8 (σ Dra, K0, $B-V = 0.79$, and 61 Cyg A, K5, $B-V = 1.18$), it is impossible to draw any conclusions about the general spectral type dependence of polarization in late G, and K type dwarfs. Both 61 Cyg A and σ Dra are, however, fairly inactive stars with low Ca II emission, and accordingly they also have small degrees of polarization.

The small polarization seen in F stars at all levels of activity may be connected with their relatively shallow outer convective zones. Theoretically, shallow convective zones exhibit only minimal amounts of inhomogeneity in their active region distribution (Giampapa and Rosner 1984). Since both the relative depth of the convective envelope and the photospheric gas pressure increase toward later spectral types, surface inhomogeneities and the photospheric magnetic field, $B_{\rm phot}\{\propto[8\pi P_{\rm gas}(\tau = 1)]^{0.5}$; Saar and Linsky 1986$\}$ will probably also increase. Increased surface inhomogeneity and $B_{\rm phot}$ lead directly to larger values of P_s, explaining the rise in polarization with color $B-V$. But while the distribution, structure and strength of magnetic fields may depend on the depth of the convective envelope and the photospheric properties, the fraction of the stellar surface covered by magnetic regions (filling factor) appears to increase with stellar rotation (Saar and Linsky 1986). We therefore expect a P_s versus $B-V$ diagram to show an envelope, growing with increasing $B-V$.

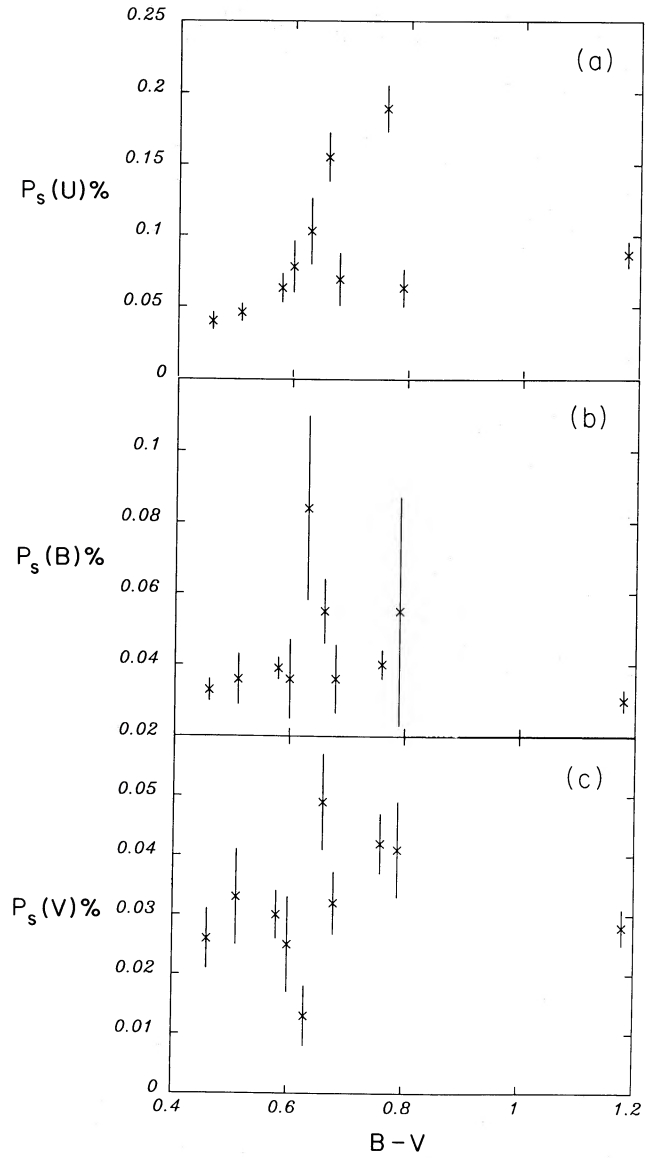

FIG. 4.—P_s (U, B, and V) vs. ($B-V$) color

The upper limit at each $B-V$ value would be occupied by stars with favorable magnetic geometries (i.e., stars with optimal combinations of the filling factor and degree of inhomogeneity for producing a net P_s signal). Note that these stars, however, would *not* inevitably be the most "active" in the traditional sense. Stars below the upper limit would then either be old and inactive, with very small filling factors of active regions, or young and active, with a number of active regions always visible and causing partial cancellation in disk-integrated polarization.

c) *Wavelength Dependence of Polarization*

Rayleigh scattering (RS), with a wavelength dependence λ^{-4}, has been suggested as one of the possible sources of linear polarization in late-type stars (Piirola and Vilhu 1982). While the correlations of P_s with magnetic activity indicators (Ca II flux and R_0; § III*a*) suggest a magnetic origin for the polarization, the wavelength dependence of P_s provides another test. Saturation in the transverse Zeeman effect (i.e., magnetic intensification, MI) causes a wavelength dependence varying from λ^{-8} (M0 dwarfs) to λ^{-3} (late F dwarfs; Saar and Huovelin 1988). It should therefore be possible to distinguish the source of the polarization by studying P_s in different passbands. We computed the wavelength dependence of polarization by fitting a power law, $P_s \propto \lambda^{-b}$, to our observations in U, B, and V (see Table 4). A similar fit was already used by Huovelin *et al.* (1985) for average values of polarization ($\langle P \rangle$) in $UBVR$. Using the improved parameter for polarization (P_s), we obtain a more accurate description of the true wavelength dependence.

The observed wavelength dependence of P_s varies from $\lambda^{-0.9\pm0.7}$ (HD 194012) to $\lambda^{-5.9\pm0.6}$ (ξ Boo A), with three stars (9 Cet, ρ CrB, and 61 Cyg A) showing exponents within 1 σ of -4 (RS). However, the exponent becomes more negative with increasing P_s in the U band. This behavior suggests that the power-law slopes may be underestimated for small overall values of P_s due to observational uncertainties such as noise which leads to overestimates of $P_s(B)$ and $P_s(V)$ (see § III*a*). We suggest, therefore, that the wavelength dependence for all stars, except 9 Cet, ξ Boo A, and HD 126053, should be taken as rough lower limits. In the case of 9 Cet and HD 126053, the expected slopes for MI and RS are both within 1 σ limits of the observed slopes, yielding ambiguous results as to the source of polarization. The only individual star with strong evidence for MI is ξ Boo A, with an observed wavelength dependence ($\lambda^{-5.9}$) significantly closer to MI ($\lambda^{-4.9}$) than to RS (λ^{-4}). We note that the actual power-law slopes for MI are probably more negative than the theoretical values given here, since the slopes have been derived using an approximation which results in a rough upper limit to the wavelength dependence (Saar and Huovelin 1987). The actual slopes depend on the average line strengths (η_0) in each passband. The difference in the exponent is less than one for reasonable values of η_0.

Comparing the average slope for stars earlier than G2 with that of stars of later spectral types provides additional support for the MI polarization mechanism. Both subsamples contain five stars and both contain small [$P_s(U) < 0.1\%$] and large polarization ($>0.1\%$) stars. Thus there should not be any major errors due to selection effects. We find the average slope for the former subsample to be $\lambda^{-1.89}$, while for the latter we obtain $\lambda^{-3.66}$. This is another argument against RS, since Rayleigh scattering should have the same wavelength dependence, independent of spectral type. The atmospheric structure

TABLE 4

OBSERVED AND THEORETICAL WAVELENGTH DEPENDENCE ($P_s \propto \lambda^{-b}$) OF LINEAR POLARIZATION FOR THE PROGRAM STARS[a]

HD	b_{MI}	b	σ_b
1835	4.4	3.5	0.6
20630	4.5	1.8	0.9
25998	2.9	1.1	0.6
126053	4.2	5.1	1.0
131156A	4.9	5.9	0.6
143761	4.1	3.1	1.1
185144	5.1	1.1	0.8
194012	3.4	0.9	0.7
201091	7.9	3.8	0.6
206860	4.0	1.9	0.6

[a] b_{MI} is the theoretical value for magnetic intensification, and σ_b is the (1 σ) error of observed b.

of single late-type dwarfs also argues for magnetic intensification (MI) as the cause for the observed linear polarization. Cool dwarfs show little evidence for the extended dust or gas envelopes which could cause Rayleigh scattering. Finally, linear polarization observed in solar active regions is certainly due to MI, and by analogy we may expect the same to be true for solar-like stars.

d) Temporal Variations

We next analyze the nearly simultaneous polarimetric and Ca II emission observations of ξ Boo A and HD 206860. HD 194012 did not show significant variations during the observing period, and for the other program stars (HD 1835, HD 20630, HD 25998, HD 126053, HD 143761, HD 185144, and HD 201091), the polarimetric and Ca II emission observations did not overlap for sufficiently long time intervals to permit meaningful comparisons. Their polarimetric variations will be discussed in a forthcoming paper (Huovelin *et al.* 1988). In the following, the criteria for "indicative" and "significant" variability are min $(X + 2\sigma_x) <$ max $(X - 2\sigma_x)$, and min $(X + 3\sigma_x) <$ max $(X - 3\sigma_x)$, respectively, X being either P, P_x, P_y, or the S-index. The Julian Dates are all JD $-2{,}440{,}000$.

Due to the time difference between Crimea and Mount Wilson, the observations were not quite simultaneous. The Ca II emission observations of ξ Boo A were made 7.7–9.1 hr later than the polarimetric observations, while the time offset of HD 206860 observations was 9.8–11.8 hr. The Ca II excess fluxes, and polarization observations are plotted against Julain Dates in Figures 5 and 6.

We computed the rotational phase for each observation, using the periods in Noyes *et al.* (1984), which are 6.2 days for ξ Boo A, and 4.7 days for HD 206860. These periods are confirmed by our own period analysis of the Ca II data at hand, kindly provided by S. Baliunas. The zero phase was defined to be the average maximum phase of Ca II emission during an interval covering the periods of polarimetric observations and long enough to extend over several rotational periods. The interval and number of observations were JD 6585–6620 and 25 for ξ Boo A, and JD 6275–6305 and 22 for HD 206860, respectively. The resulting time for zero phase for ξ Boo A was JD 6595.7, and for HD 206860 we obtained JD 6281.0. The Ca II excess fluxes versus phase are plotted in Figure 7. We advise against interpreting any general ephemeris for either star from these results, since the phase of maximum for Ca II emission can change considerably on time scales as short as a few months, presumably due to the growth and decay of active regions. The mainly qualitative results of our study are as follows.

ξ Boo A (HD 131156A).—Polarimetric variations during the five nights in JD 6599–6604 were significant in $P_x(V)$, while being indicative in $P(U)$, $P(B)$, $P_x(U)$, and $P_x(B)$. The small variations in P_y (UBV) are due to the polarization being directed close to the north-south axis (in equatorial coordinates). The Ca II emission observations were extensive, covering 163 nights in JD 6157–6640. The overall variations were large and well above the significant level. During the five nights of polarimetry, the Ca II emission variations were also significant, allowing reasonable comparisons with polarimetric variations (see Fig. 8*a*).

The variations of Ca II emission in ξ Boo A (see Figs. 7*a* and 8*a*) suggest active areas in more than one longitude, since stellar surface with only one active region could not generate the smaller maximum, roughly at phase 0.2–0.3. We estimate the approximate longitudes of the active regions using an elementary spot model. The Ca II emission from each spot was assumed to be time-independent, with variations exclusively due to changes in projected area and limb darkening. A fixed

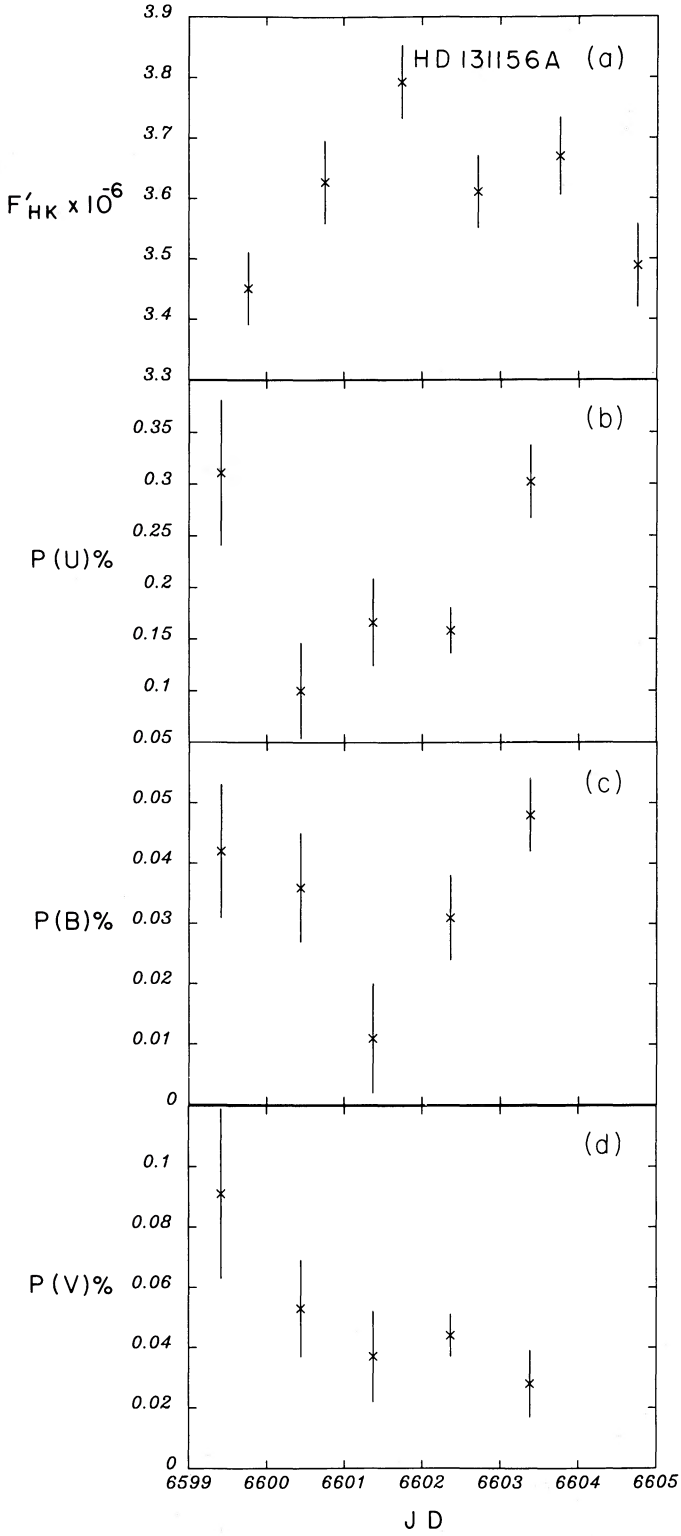

FIG. 5.—(*a*) Ca II flux, and degree of polarization (*b*), (*c*), and (*d*) vs. Julian date for HD 131156A (ξ Boo A).

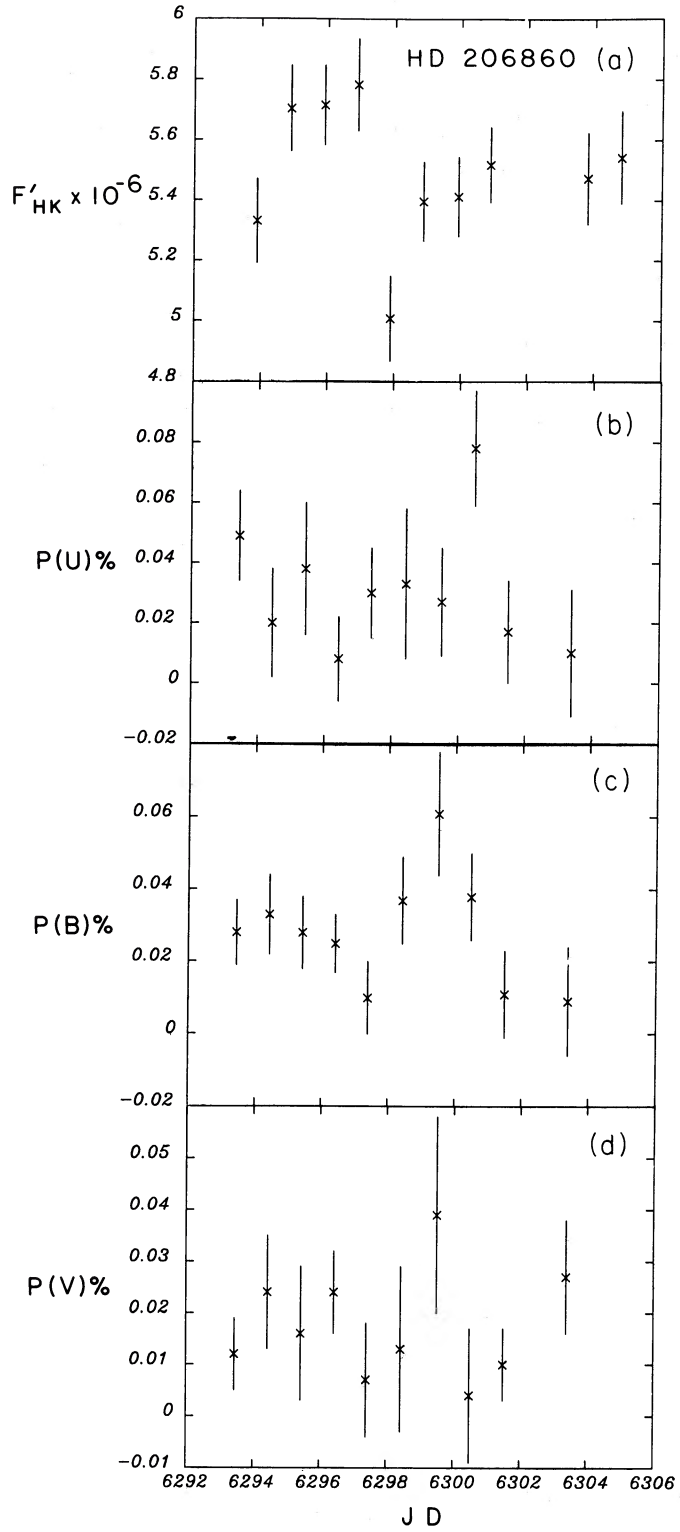

FIG. 6.—As Fig. 5, but for HD 206860

background flux due to chromospheric network was included. We also assumed the spot areas were small (i.e., one surface element) and allowed the disk center intensity of emission to be a free parameter for each spot. While the model is unrealistic in some ways (e.g., it does not account for the finite areas and latitudes of the spots), it is probably adequate for rough estimates of surface geometries and has few free parameters. We fitted a two-spot model to the observations, using the limb-darkening law for Ca II (H + K) line core emission from Skumanich *et al.* (1984), and assumed that both spots were equatorial. We then compared the resulting spot locations with the polarimetry. Linear polarization (in *U* and *B*) was smaller near zero phase (primary spot face-on), and larger at phase 0.25 (see Figs 8*b*, 8*c*, and 8*d*), roughly agreeing with the model. Polarization, however, was also enhanced at phase 0.6, when both spots (secondary trailing the primary with 115° difference) should have been behind the disk. We therefore added a third spot to the model. In this case, the model failed to converge to unique estimates for the spot longitudes, finding significantly different solutions depending on the arbitrarily chosen minimum flux. The large polarization at phase 0.6, if real (there were only two observations on that night), suggests the presence of a third smaller active area, clearly separated from the two primary areas.

One interesting feature of the data was the constancy of the direction of polarization in ξ Boo A during the entire observing run. The average polarization angle (with a 180° ambiguity) was 175° ± 4° in the *U* band, and 175° ± 7° in the *B* band, the ranges of variations being from 171° to 186°, and 169° to 194°, in *U* and *B*, respectively. This result sets some limits on the active area configuration. From the ξ Boo A + B binary orbital elements (Aitken 1964), we infer the projected orbital axis of the system on the plane of the sky to be 78°.3, measured counterclockwise from the north pole direction, while the orbital inclination (i.e., the angle between the orbital plane and

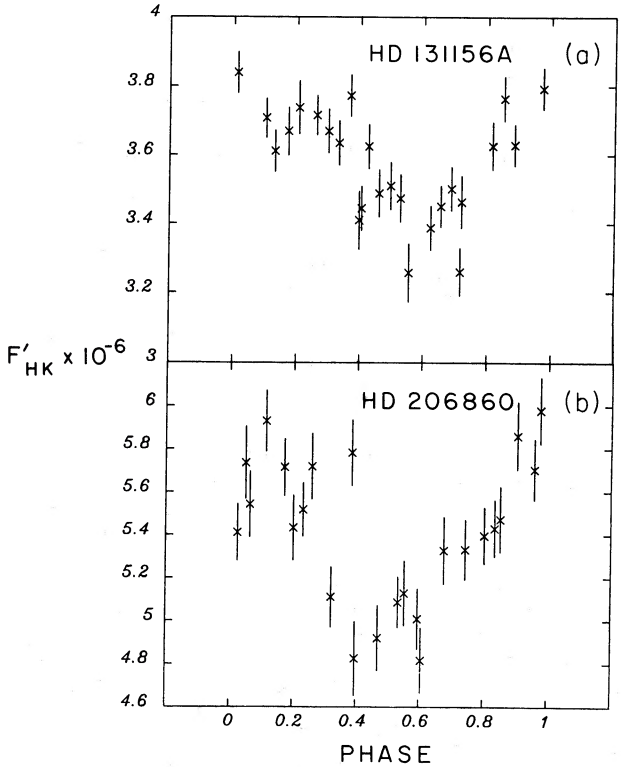

FIG. 7.—(*a*) Ca II emission in HD 131156A (JD 6585–6620) vs. rotational phase. Zero phase was JD 6595.7, and period $6^d.2$ (*b*) HD 206860, (JD 6275–6305), zero phase JD 6281.0, and period $4^d.7$.

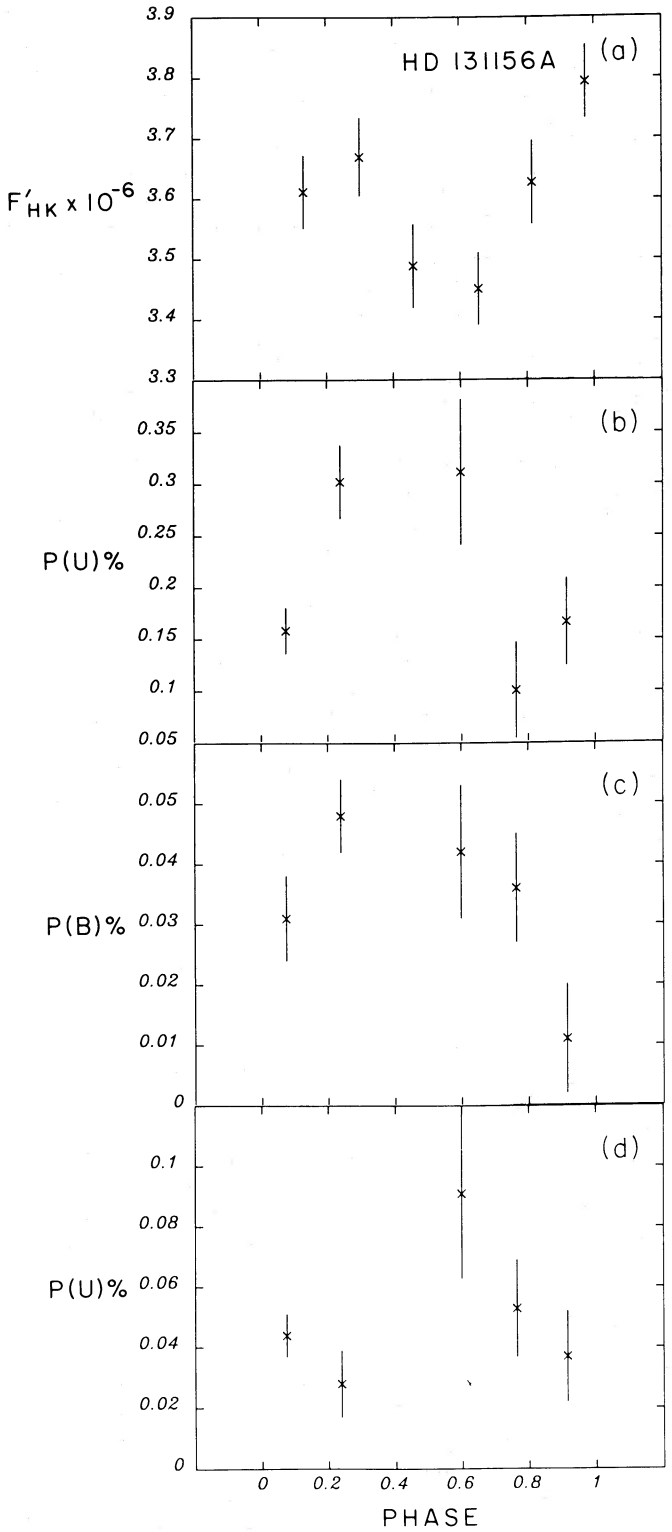

FIG. 8.—Observations of Fig. 5 (HD 131156A) vs. rotational phase

the plane of the sky) is 40°. We can compare this value to the stellar inclination derived from estimates of $v \sin i$, the rotation period, and the radius of ξ Boo A. Taking $v \sin i = 4 \pm 1.5$ km s^{-1}, $P_{rot} = 6.2 \pm 0.2$ days, and $R/R_{\odot} = 0.9 \pm 0.1$, we obtain an average $i = 35°$ (with a range from 18° to 66°), in agreement with the orbital inclination. Assuming that the orbital and stellar rotation axes are identical, the observed polarization cannot be explained by an active region close to the pole, since the polarization angle (0° or 180°) is not close to the axis direction (78°). Instead, magnetic regions which pass close to disk center during rotation will exhibit the minimum deviations from the 0°/180° polarization angle. Thus, several active areas at intermediate latitudes ($\sim 55°$), spaced in phase as indicated by the Ca II data, could produce the observed polarimetric variations.

HD 206860.—During the nearly simultaneous observations (10 nights in JD 6293–6304), significant variations were observed in $P_x(V)$, and $P_y(U)$, while variations in $P(U)$, $P_x(B)$, and $P_y(U)$ were indicative. The Ca II emission measurements covered 50 nights in JD 6278–6375, showing significant overall variability, and from less than indicative to significant variations in six night subintervals. During the period of overlapping polarimetric and Ca II emission observations, variation in Ca II emission was close to significant (2.6 σ).

The Ca II emission of HD 206860 also shows two peaks (with the secondary peak at phase ~ 0.1; Figs. 7*b* and 9*a*), suggesting two active areas with about 40° longitudinal separation if at the equator. An elementary two-spot model confirms the separation. The enhancement of Ca II emission in JD 6696.9 (near phase 0.4), however, contradicts the two-spot model. One period of rotation earlier, the enhancement was not present, and a period later the star was not observed. Thus, the active area causing this variation formed during the observing period. The enhancement of $P(U)$ near phase 0.15 (Fig. 9*b*) is consistent with the primary active area (assumed equatorial) being in optimum location for polarization (55°). A small increase in $P(U)$ was observed also at phases 0.6–0.7. $P(B)$ showed small increases as well, following trends in the U band (Fig. 9*c*). The increase observed between phases 0.6 and 0.7 may therefore be real, suggesting smaller active areas $\sim 180°$ behind the leading active area (agreeing roughly with the Ca II emission enhancement at phase ~ 0.4). The most prominent enhancement in $P(B)$, however, occurred at phase 0.95. This agrees well with the secondary active area location (about 0.20 at phase before passage through disk center), but the lack of a simultaneous significant increase in $P(U)$ is unexplained. During the observations, $P(V)$ did not show significant variability (Fig. 9*d*).

In summary, the surface distribution of active areas on HD 206860 consisted of two major areas, separated by about 40° in longitude, and smaller regions at the opposite side of the star. The actual sizes of the regions cannot be derived from the data, but the Ca II emission variations suggest that the two major areas were of nearly equal size.

IV. CONCLUSIONS AND SUGGESTIONS FOR FUTURE WORK

Our observations indicate that linear polarization in late-type dwarfs is related to chromospheric Ca II emission, albeit in complex ways. The choice of parameters is crucial in studies of the relations between long-term averages, and the conventional vectorial average of linear polarization $\langle P \rangle = (\langle P_x \rangle^2 + \langle P_y \rangle^2)^{0.5}$ is unsuitable for rotationally modulated linear polarization. Instead, a scalar average of the polarization degree $P_s = \langle (P_x^2 + P_y^2)^{0.5} \rangle$ is a more suitable parameter, provided that significant deviations from zero (i.e., above the noise) are present. Ca II fluxes in relative units (i.e., units of R_{HK}') correlate better with P_s than Ca II fluxes in absolute units, undoubtedly because polarization (by definition) is also given in relative units.

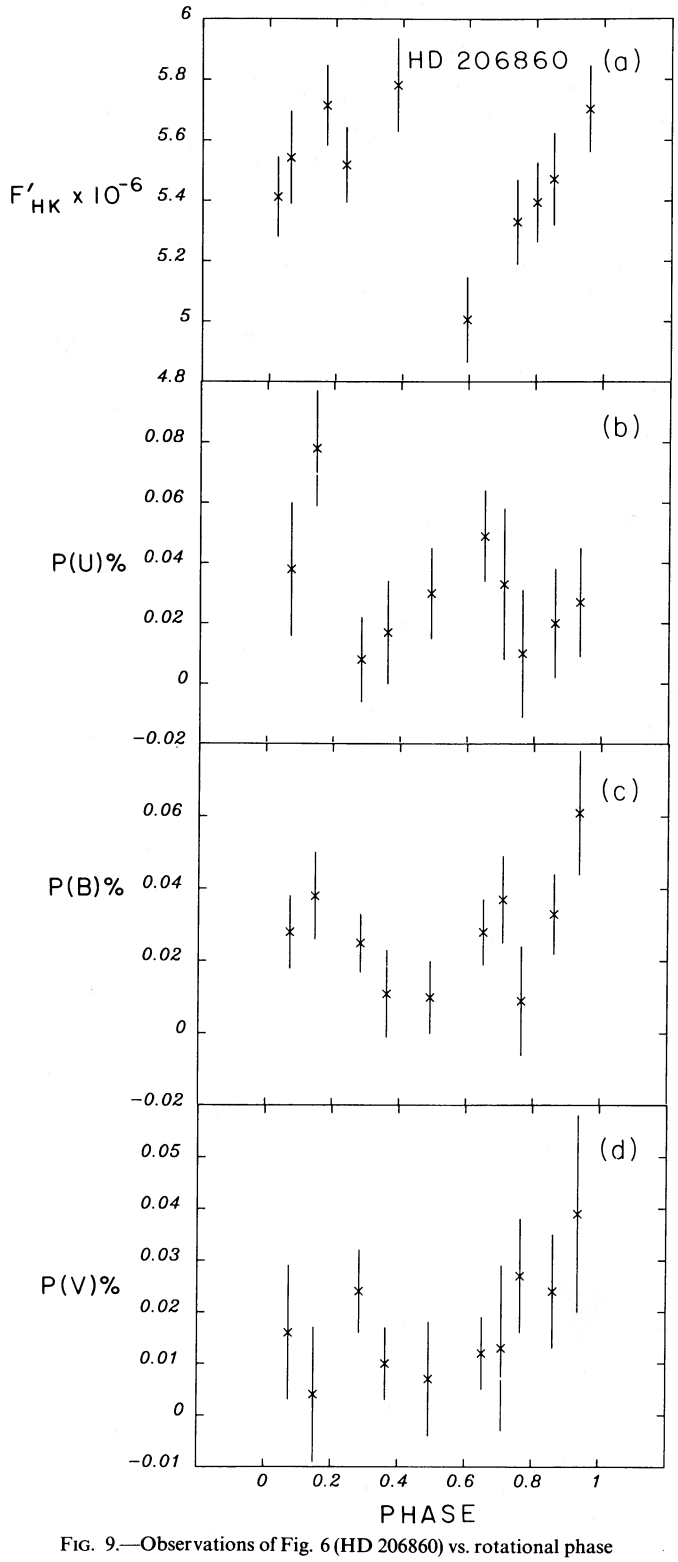

FIG. 9.—Observations of Fig. 6 (HD 206860) vs. rotational phase

There is possibly a weak increase in linear polarization with R_{HK}' and with the inverse Rossby number R_0 (Figs. 1 and 2). The scatter in the relations is, however, large. The increase in linear polarization with R_{HK}' and R_0 is most significant in the U band, partly because observational uncertainties (the uncertainty in the zero point is particularly important) may affect the smaller polarization values in B and V. The scatter in the linear polarization versus chromospheric activity (Figs. 1 and 2) can be understood by considering the complicated relations between magnetic field strength, area distribution and linear polarization. The disk-integrated degree of linear polarization is an ambiguous activity indicator, since it can be equally small in both active stars with large numbers of magnetic regions widely spaced on their surface (due to cancellation effects), and in stars with relatively low activity.

The increase of broadband linear polarization in the ultraviolet with $B-V$ color (Fig. 4*a*) indicates an increase in the field strength and/or inhomogeneity of magnetic areas toward later spectral types. There is empirical evidence for both the former suggestion in late-type dwarfs (Saar and Linsky 1986), and theoretical evidence for the latter (Giampapa and Rosner 1984). In particular, magnetic regions in F dwarfs may be fairly small in size and more homogeneously distributed (Giampapa and Rosner 1984), leading to generally small values of linear polarization independent of the stellar magnetic activity level. Our data on F stars are completely consistent with this idea. For later spectral types we see the range in the degree of polarization increase, probably indicating the range of filling factors and geometries at each spectral type.

All of the program stars show the largest polarization in the U band. The wavelength dependence of the average linear polarization (P_s) varies with spectral type and also generally shows steeper slopes in stars with larger polarization. Qualitatively, the observed wavelength dependence could have at least two explanations: (1) The increase in the number of saturated, Zeeman-sensitive absorption lines toward the blue can produce net linear polarization via the magnetic intensification mechanism, or (2) Rayleigh scattering in the optically thin parts of the stellar atmosphere. The observed scatter in the wavelength dependencies and their trend with $B-V$, however, support the magnetic intensification hypothesis, as do the increase of linear polarization with $B-V$ in the U band (Fig. 4*a*) and the weak trend in Ca II (H + K) emission (Figs. 1 and 2), agreeing with observations of net linear polarization in solar magnetic regions. Of course, other phenomena that might cause linear polarization in magnetic regions are not excluded by this result.

The interpretation of simultaneous rotational variations in Ca II emission and broad-band linear polarization is difficult due to the phase difference of maxima between these two quantities, and the partial cancellation in the disk-integrated polarization. The small variations in the inactive late-type dwarfs also appear to be close to the detection limits of current measurement devices. The most active G-type and K-type dwarfs, on the other hand, show significant polarimetric variations, and comparison of simultaneous changes in broad-band linear polarization with other magnetic activity indicators provides complementary information on the magnetic area distributions. The combination of polarimetric and Ca II emission observations of two such stars, ξ Boo A and HD 206860, indicates at least three active areas on both stars. The observed variations may be explained with the following rough models: two (not equally) large magnetic regions and one smaller region, equally spaced at intermediate latitudes on ξ Boo A, and two equally large equatorial regions (separated by $\sim 40°$ in longitude) with a third smaller region roughly at the opposite side of the star on HD 206860.

Broad-band polarimetry is clearly a useful tool in studies of stellar magnetic region structures, although the complicated

relations with other observations make the interpretations difficult. When planning the future polarimetric observations of main sequence stars, the following should be considered:

1. The most favorable targets are magnetically active stars, of spectral types later than F, that show significant chromospheric variability.

2. The largest polarization and variability is generally expected in the ultraviolet (U) band, while the blue (B) and the visual (V) bands usually show considerably smaller polarization levels, possibly affected by the uncertainty in the instrumental polarization.

3. The targets should be monitored for an extended time over many rotational phases, covering at least two periods of rotation.

4. Simultaneous observations of other magnetic activity indicators [e.g., Ca II (H + K) and infrared triplet emission, ultraviolet line emission, Zeeman-broadened absorption lines, and photometric variations] should be included to obtain complementary information on the spatial structure of the stellar active regions.

5. Finally, to confirm the general trends suggested in our study, a long-term observing plan should contain a selection of stars of different spectral types (G0–M) and different magnetic activity levels.

We are currently carrying out plans to monitor active late-type dwarfs with several instruments simultaneously, including observations of linear polarization, spectra, and Ca II (H + K) emission.

This work was supported by a grant from the Academy of Finland and by NASA grant NGL-06-003-057 to the University of Colorado. We thank J. Linsky for carefully reading and commenting on the manuscript, and S. Baliunas and the Mount Wilson stellar activity team for kindly providing the Ca II observations in advance of publication. J. H. and I. T. are also grateful to Professor A. A. Boyarchuk and the staff of the Crimean Observatory for the observing time and hospitality.

REFERENCES

Aitken, R. 1964, *The Binary Stars* (New York: Dover), p. 286.
Baliunas, S. L., *et al.* 1983, *Ap. J.*, **275**, 752.
Böhm-Vitense, E. 1981, *Ann. Rev. Astr. Ap.*, **19**, 295.
Calamai, G., Landi Degl'Innocenti, E., and Landi Degl'Innocenti, M. 1975, *Astr. Ap.*, **45**, 297.
Dollfus, A. 1958, *C. R. Acad. Sci., Paris*, **246**, 3590.
Giampapa, M., and Rosner, R. 1984, *Ap. J. (Letters)*, **286**, L19.
Hsu, J., and Bregel, M. 1982, *Ap. J.*, **262**, 732.
Huovelin, J., Linnaluoto, S., Piirola, V., Tuominen, I., and Virtanen, H. 1985, *Astr. Ap.*, **152**, 357.
———. 1986, in *Cool Stars, Stellar Systems, and the Sun*, ed. M. Zeilik and D. M. Gibson (New York: Springer), p. 333.
Huovelin, J., Linnaluoto, S., Tuominen, I., and Virtanen, H. 1988, in preparation.
Kemp, J. C., and Wolstencroft, R. D. 1974, *M.N.R.A.S.*, **166**, 1.
Landi Degl'Innocenti, E. 1982, *Astr. Ap.*, **110**, 25.
Landi Degl'Innocenti, M., Calamai, G., Landi Degl'Innocenti, E., and Patriarchi, P. 1981, *Ap. J.*, **249**, 228.
Leroy, J. L. 1962, *Ann. d'Ap.*, **25**, 127.
Noyes, R. W., Hartmann, L., Baliunas, S. L., Duncan, D. K., and Vaughan, A. H. 1984, *Ap. J.*, **279**, 793.
Piirola, V. 1973, *Astr. Ap.*, **27**, 383.
———. 1975, *Ann. Acad. Sci. Fennicae*, **A VI**, No. 418.
———. 1977, *Astr. Ap. Suppl.*, **30**, 213.
Piirola, V., and Vilhu, O. 1982, *Astr. Ap.*, **110**, 351.
Rutten, R. 1984, *Astr. Ap.*, **130**, 353.
Saar, S. H., and Huovelin, J. 1988, in preparation.
Saar, S. H., and Linsky, J. L. 1986, *Adv. Space Phys.*, Vol. **6**, No. 8, p. 235.
Schrijver, C. J. 1988, *Astr. Ap.*, **189**, 163.
Schrijver, C. J., Coté, J., Zwaan, C., and Saar, S. H. 1988, *Astr. Ap.*, submitted.
Skumanich, A., Lean, J. L., White, O. R., and Livingston, W. C. 1984, *Ap. J.*, **282**, 776.
Tinbergen, N., and Zwaan, C. 1981, *Astr. Ap.*, **101**, 223.
Unno, W. 1956, *Pub. Astr. Soc. Japan*, **8**, 108.
Vaughan, A. H., Baliunas, S. L., Middelkoop, F., Hartmann, L., Mihalas, D., Noyes, R. W., and Preston, G. 1981, *Ap. J.*, **250**, 276.
Vaughan, A. H., Preston, G. W., and Wilson, O. C. 1978, *Pub. A.S.P.*, **90**, 276.

JUHANI HUOVELIN and ILKKA TUOMINEN: Observatory and Astrophysics Laboratory, University of Helsinki, Tähtitorninmäki, SF-00130 Helsinki, Finland

STEVEN H. SAAR: Harvard-Smithsonian Center for Astrophysics, Mail Stop 58, 60 Garden Street, Cambridge, MA 02138